EUROPEAN ORGANIZATION FOR NUCLEAR RESEARCH

CERN-PPE/96-152
October 25, 1996

Search for Exclusive B Decays to J and η or π^0 with the L3 Detector

The L3 Collaboration

Abstract

A search for exclusive decays of B_d^0 and B_s^0 mesons has been performed in the channels $B_d^0 \to J\eta$, $B_s^0 \to J\eta$, $B_d^0 \to J\pi^0$ and $B_s^0 \to J\pi^0$. The data sample consisted of more than three and half million hadronic Z decays collected by the L3 experiment at LEP from 1991 through 1995. No candidate events have been observed for any of the modes thus determining upper limits at 90% confidence level: 3.2×10^{-4} on $\mathrm{Br}(B_d^0 \to J\pi^0)$ and the first experimental limits:

$$\begin{aligned} \mathrm{Br}(B_d^0 \to J\eta) &< 1.2 \times 10^{-3}, \\ \mathrm{Br}(B_s^0 \to J\eta) &< 3.8 \times 10^{-3}, \\ \mathrm{Br}(B_s^0 \to J\pi^0) &< 1.2 \times 10^{-3}. \end{aligned}$$

Submitted to *Phys. Lett. B*

Introduction

The high statistics data collected at the Z peak by the LEP experiments allow the study of rare B physics processes such as colour suppressed exclusive B decays to charmonium states.

This paper describes the search for hadronic decays of B_d^0 and B_s^0 meson and their charge conjugates to J plus a light pseudoscalar meson in the exclusive modes $B_d^0 \to J\eta$, $B_d^0 \to J\pi^0$ and $B_s^0 \to J\eta$. The full data sample collected in the years from 1991 through 1995 with the L3 detector has been used, corresponding to more than three and half million hadronic decays of the Z. J's have been detected by means of their decay into electron or muon pairs and η's and π^0's through their decay into photon pairs, exploiting the L3 detector performances in detecting these particles.

These exclusive decay modes are expected to proceed through the diagrams in Figure 1. The only previous existing result on these decay modes is the 90% confidence level upper limit on $\mathrm{Br}(B_d^0 \to J\pi^0)$ set by the CLEO collaboration as 6.9×10^{-5} [1].

B decays to charmonium are believed to be dominated by colour suppressed mechanisms. Penguin diagrams are suppressed since two or even three gluons are needed to form a charmonium state [2]. The decays under investigation thus provide a clean environment for the study of colour suppressed processes. Moreover, these decays constitute an interesting test of the factorization approach to the description of two body decays of B mesons. The predictions for the branching ratios of the processes under study range from $(1.0 \pm 0.4) \times 10^{-3}$ for $B_s \to J\eta$ down to $(1.0 \pm 0.4) \times 10^{-5}$ for $B_d \to J\eta$ as in References [3].

Factorization has been proposed by Feynman [4] in 1964 in the investigation of hyperon decay, and since then it has been successfully applied to the description of processes involving strange and charmed particles. In more recent times the factorization hypothesis has been used in order to investigate the weak hadronic decay of charmed and beauty mesons (cfr. [5] and references therein). As summarized, for example, in Reference [6], the currently used factorization approach fails to explain simultaneously the branching ratio with respect to $B_d^0 \to JK^0$ and the polarisation of $B_d^0 \to JK^*$ decay as measured by ARGUS [7], CDF [8] and CLEO [9] collaborations.

The possible presence of a non-factorized term in the description of B decay amplitude has been proposed in [10] as a solution to this problem, and the size of this term has been analysed in [11] for B decays to a J plus a pseudoscalar meson. Large values of the branching ratios of the processes under study could result from this non-factorized term.

The $B_s^0 \to J\pi^0$ mode, which is not described by the diagrams in Figure 1, has been searched for as well.

The L3 detector

The L3 detector consists of a silicon microvertex detector, a central tracking chamber, a high resolution bismuth germanium oxide (BGO) crystal electromagnetic calorimeter, a ring of plastic scintillation counters, a uranium and brass hadron calorimeter with proportional wire chamber readout, and an accurate muon chamber system. These detectors are installed in a 12 m diameter magnet which provides a uniform field of 0.5 T along the beam direction. Luminosity is measured with forward BGO arrays on each side of the detector. A detailed description of each detector subsystem and its performance is given in Reference [12].

The subdetectors most relevant for this analysis are the central tracking chamber, the electromagnetic calorimeter and the muon spectrometer. The central tracking chamber is a time expansion chamber (TEC) which consists of two cylindrical layers of 12 and 24 sectors, with wires measuring the R-ϕ coordinate in a plane normal to the beam direction. The z coordinate is measured by a Z-chamber mounted just outside the TEC.

The electromagnetic calorimeter, placed around the TEC, consists of 10 734 BGO crystals arranged in two half-barrels with polar angle coverage $42^\circ \leq \theta \leq 138^\circ$ (where θ is defined with respect to the beam axis) and two endcaps covering $10^\circ \leq \theta \leq 38^\circ$ and $142^\circ \leq \theta \leq 170^\circ$. The energy resolution of the BGO calorimeter is $\simeq 5\%$ for photons and electrons with energies around 100 MeV and is less than 2% for energies above 1 GeV. The angular resolution of electromagnetic clusters is better than 0.5° for energies above 1 GeV.

The muon spectrometer consists of three layers of precise drift chambers for the measurement of the transverse momentum of the muon. The inner and outer muon chambers are surrounded with additional layers of drift chambers allowing the measurement of the the polar angle. For muons of 45 GeV the three chamber layers allow a momentum measurement with a resolution of 2.5%. The polar angle measurement has a precision of 4.5 mrad which is dominated by multiple scattering of the muon in the calorimeters, while the resolution on the radial angle is of the order of 1 mrad. The polar angle coverage of this spectrometer considered in this analysis extends from 36° to 144°.

The mass resolutions achieved with the L3 detector in the η reconstruction from photon pairs is 17.8 MeV [13] and the ones for J from muons and electrons pairs are 122 MeVand 83 MeV [14], respectively.

Event simulation

The JETSET 7.4 [15] Monte Carlo, based on the Lund parton shower model, was used to generate a total of 40 000 $\mathrm{Z} \rightarrow \mathrm{b\bar{b}}$ events, 5 000 events in each of the exclusive decay modes: $\mathrm{B_d^0} \rightarrow \mathrm{J}\eta$, $\mathrm{B_d^0} \rightarrow \mathrm{J}\pi^0$, $\mathrm{B_s^0} \rightarrow \mathrm{J}\eta$ and $\mathrm{B_s^0} \rightarrow \mathrm{J}\pi^0$, with the subsequent decay of the J into a muon or electron pair and of η's and π^0's into photon pairs.

The b quark on the other side of the event was left free to hadronize and decay. The masses of the generated $\mathrm{B_d^0}$ and $\mathrm{B_s^0}$ mesons were 5.279 GeV and 5.373 GeV, respectively. The events were then passed through the full L3 simulation which takes into account the effects of energy loss, multiple scattering, interactions and decays in the detector materials. This simulation is based on the GEANT package [16] with the GHEISHA [17] program for the simulation of hadronic interactions. Inefficiencies of the various subdetectors, as obtained from the data, were also simulated. These events, after reconstruction by the same program used for the data, were used to tune the analysis procedure and calculate the efficiency of the event selection criteria.

Background processes consisting of combinatorics and misidentification of photons, π^0's and leptons were studied using hadronic decays of the Z generated with the JETSET Monte Carlo and passed through the detector simulation and reconstruction chain described above. The hadronization of the light quarks was described by the Lund symmetric fragmentation function [15] while the Peterson fragmentation function [18] was used to describe the fragmentation of the c and b quarks. The mean value of the ratio of the energy of the weakly decaying B hadron to the beam energy used in the generation was $\langle x_\mathrm{E} \rangle = 0.703$.

Event selection

Since the hard fragmentation of the b quark gives on average 70% of the beam energy to the B_d^0 or B_s^0 meson, the η/π^0's are likely to have high momentum and their two decay photons can have a small opening angle. Thus the neutral light hadrons can give a single energy cluster in the electromagnetic calorimeter. This analysis has been performed in four different final state configurations, which give the best acceptance and background rejection capability as from the Monte Carlo simulations described in the previous section:

- $B_{d,s}^0 \to J\eta \to e^+e^-\gamma\gamma$,
- $B_{d,s}^0 \to J\eta \to \mu^+\mu^-\gamma\gamma$,
- $B_{d,s}^0 \to J\pi^0 \to e^+e^-$cluster,
- $B_{d,s}^0 \to J\pi^0 \to \mu^+\mu^-$cluster.

Four sets of event observables have been used to identify photon pairs from η, electromagnetic clusters from π^0, muons and electrons. These variables and the selection criteria on their values are described in the following and summarized in Table 1.

- The photons used for the reconstruction of the η were selected from clusters in the full BGO calorimeter angular coverage which had lateral shower shapes consistent with electromagnetic energy depositions, as measured by an estimator, χ^2_{em}, that takes into account the expected behaviour crystal by crystal as from test beam data. A requirement on the opening angle (θ_{3D}) between each photon candidate and the closest track in the TEC was also applied. A minimum energy ($E_{cluster}$) and a minimum number of crystals were finally required. The η's have been reconstructed from photon pairs by imposing requirements on their invariant mass ($M_{\gamma\gamma}$) and opening angle ($\theta_{\gamma\gamma}$). In addition, a cut on the cosine of the angle between the direction of the reconstructed η in the $B_{d,s}^0$ candidate rest frame and the $B_{d,s}^0$ candidate flight direction in the laboratory frame (θ^*) has been used.

- The selection of the single clusters from π^0 decays placed requirements on the number of crystals in the shower, χ^2_{em}, θ_{3D} and $E_{cluster}$, such as in the search for photons from the η decays. The single clusters from π^0 decays are expected to have relatively high energies since the opening angle between the two photons is small enough so as not to resolve them. This strategy for the selection of the π^0's, already applied in Reference [19], can in principle increase the background in the final mass window.

- Muons were identified by requiring a track segment in at least two of the muon chamber layers in the plane transverse to the beam axis and in one of the chambers in the longitudinal plane. The reconstructed tracks needed to satisfy a minimum momentum requirement (different for the lower and higher energetic muon momenta, $p_\mu^{(1)}$ and $p_\mu^{(2)}$, respectively) and to point toward the event vertex both in the transverse and longitudinal planes, as measured by the distances V_{xy} and V_z from the vertex, given their resolutions σ_{xy} and σ_z.

- Electrons were identified by requiring electromagnetic showers with a minimum number of crystals and energy, where $E_e^{(1)}$ and $E_e^{(2)}$ in Table 1 denote the energies of the lower and higher energy clusters, respectively. These showers had to be isolated as measured by the ratio of the energy deposition in a 3×3 to a 5×5 crystal matrix centered on the most energetic crystal of the cluster (Σ_9/Σ_{25}). A charged track which fulfilled some quality requirements and close enough (θ_{3D}) to the cluster was required to be associated with it by means of an estimator which compares the transverse momentum (p_T) of the track and the energy of the cluster in the transverse plane (E_T) given the resolutions (σ_T) on this quantity.

No difference between the B^0_d and B^0_s mesons was made throughout this phase of the analysis. Different thresholds for the reconstructed $B^0_{d,s}$ meson energy (E_B) were required for the π^0 and η channels since reconstruction of a resolved η favours a lower energy $B^0_{d,s}$. The J candidates were reconstructed by requiring an opposite charge muon or electron pair with opening angle less than 90° and an invariant mass ($M_{e^+e^-}$ or $M_{\mu^+\mu^-}$) consistent with different J mass ranges for the two leptons. A cut on the angle Θ_J between the direction of the reconstructed J and the neutral light hadron was also applied, as shown in Table 1.

	Variable	Preselection	Loose cuts	Final cuts
η	$E_{cluster}$	> 0.1 GeV	> 0.1 GeV	> 0.1 GeV
	χ^2_{em}	< 15	< 10	< 6
	θ_{3D}	> 10 mrad	> 20 mrad	> 20 mrad
	E_B	-	> 10 GeV	> 15 GeV
	$M_{\gamma\gamma}$ range	$(0.4, 0.7)$ GeV	$(0.495, 0.605)$ GeV	$(0.51, 0.59)$ GeV
	$\cos\theta^*$	-	-	> -0.775
	$\theta_{\gamma\gamma}$	$< 90°$	$< 60°$	$< 40°$
π^0	$E_{cluster}$	> 3 GeV	> 3 GeV	> 5 GeV
	χ^2_{em}	< 35	< 15	< 8
	θ_{3D}	> 10 mrad	> 30 mrad	> 30 mrad
	E_B	-	> 10 GeV	> 20 GeV
$J \to \mu^+\mu^-$	V_{xy}/σ_{xy}	< 4	< 4	< 4
	V_z/σ_z	< 4	< 4	< 4
	$p^{(1)}_\mu$	> 2.0 GeV	> 2.5 GeV	> 2.5 GeV
	$p^{(2)}_\mu$	> 2.0 GeV	> 4.5 GeV	> 4.5 GeV
	$M_{\mu^+\mu^-}$ range	$(2.0, 4.0)$ GeV	$(2.7, 3.5)$ GeV	$(2.85, 3.35)$ GeV
	Θ_J	$< 90°$	$< 60°$	$< 40°$
$J \to e^+e^-$	χ^2_{em}	< 15	< 10	< 10
	θ_{3D}	< 50 mrad	< 25 mrad	< 25 mrad
	$\lvert 1/E_T - 1/p_T \rvert/\sigma_T$	< 5	< 1	< 1
	Σ_9/Σ_{25}	> 0.6	> 0.8	> 0.8
	$E^{(1)}_e$	> 0.5 GeV	> 0.5 GeV	> 0.5 GeV
	$E^{(2)}_e$	> 0.5 GeV	> 0.5 GeV	> 5 GeV
	$M_{e^+e^-}$ range	$(2.0, 4.0)$ GeV	$(2.7, 3.5)$ GeV	$(2.9, 3.3)$ GeV
	Θ_J	$< 90°$	$< 60°$	$< 40°$

Table 1: The four sets of requirements used to identify η, π^0, $J \to \mu^+\mu^-$ and $J \to e^+e^-$ candidates. Definitions of the variables are given in the text. Preselection requirements, loose and final cuts are listed.

The optimization of the cuts proceeded as follows. First, a preselection, based on a set of minimal requirements, was applied: hadronic decays of the Z boson were selected as in

Reference [20] and events were required to have an opposite charge lepton pair in addition to either an energetic single cluster or a photon pair. The J and neutral light hadron candidate were required to fulfil the criteria in the third column of Table 1 and the reconstructed B mass was required to lie between 3.5 and 7.0 GeV.

The distributions of selection variables after the preselection were examined for Monte Carlo simulations of the signal and background samples to determine a set of loose cuts summarized in Table 1. Distributions of the variables for the data were also compared in order to check that the Monte Carlo described the data well. Satisfactory agreement was found, as shown in Figure 2.

The loose cuts were applied to all the variables but one. The distribution of this variable was then studied for signal and background Monte Carlo simulations, either choosing a final cut in order to reject as much background as possible, while keeping a reasonable efficiency or by using the loose cut itself as the final one. This process has been repeated for each variable. The final selection requirements which are reported in Table 1, are the same for the $\mathrm{B^0_d}$ and the $\mathrm{B^0_s}$ analyses.

Using a kinematic fit constrained to the masses of η or J, the energies and the angles of photons from η decays and of electron and muons from J decays have been refined within the resolutions of the subdetector used to measure them. This procedure has been applied to any identified η and J before the calculation of any variable of the reconstructed B system, and improves the resolution on the final reconstructed mass. This improvement ranges from 45% for the final state with a muon pair and a high energy cluster up to 90% for the final state with two electrons and two resolved photons.

Results

The four possible combinations of sets of selection requirements (η or π^0 and $\mathrm{J} \rightarrow \mathrm{e^+e^-}$ or $\mathrm{J} \rightarrow \mu^+\mu^-$) have been applied, and the invariant mass of each $\mathrm{B^0_{d,s}}$ candidate was calculated for all the decay modes. The application of the $\mathrm{J} \rightarrow \mathrm{e^+e^-}$ or $\mathrm{J} \rightarrow \mu^+\mu^-$ selections alone in the full data sample gave a little more than one hundred and nearly two hundred events respectively.

The invariant mass distribution for events surviving the cuts in the $\mathrm{B^0_d}$ and $\mathrm{B^0_s}$ signal Monte Carlo was fit with a Gaussian of width σ. The resulting resolutions are summarized in Table 2. Events in a $\pm 2\sigma$ window around the fit mass of the $\mathrm{B^0_{d,s}}$ meson were then counted in the signal Monte Carlo and in the data in order to calculate, respectively, the efficiency and the number of $\mathrm{B^0_{d,s}}$ candidates. These invariant mass spectra for the data and the Gaussian fits to the $\mathrm{B^0_d}$ and $\mathrm{B^0_s}$ Monte Carlo samples after the application of the final cuts are shown in Figure 3.

The efficiencies are given in Table 2, together with their statistical and systematic errors; the systematic errors have been estimated by analysing events generated with a harder or softer fragmentation function, *i.e.* with $\langle x_\mathrm{E} \rangle = 0.720$ or $\langle x_\mathrm{E} \rangle = 0.680$. These efficiencies do not include the branching ratio for the dilepton decay of the J and the η and π^0 decay into photon pairs. The widths and the efficiencies for $\mathrm{B^0_d}$ and $\mathrm{B^0_s}$ in the same final states are compatible, as expected from their small kinematic differences.

No candidate events have been found for any of the final state configurations in the $\mathrm{B^0_d}$ and $\mathrm{B^0_s}$ mass windows, as shown in Figure 3. Upper limits at 90% confidence level have been set using the following numerical values: $\mathrm{N_{had}} = 3\,670\,147$ as the number of Z bosons decaying to hadrons, $\Gamma_{\mathrm{b\bar{b}}}/\Gamma_{\mathrm{had}} = 0.222 \pm 0.003(\mathrm{stat.}) \pm 0.007(\mathrm{syst.})$ as the partial width of Z decays into b quarks with respect to the hadronic decays [21], $f(\mathrm{b} \rightarrow \mathrm{B^0_d}) = 39.5 \pm 4.0\%$ and $f(\mathrm{b} \rightarrow \mathrm{B^0_s}) = 12.0 \pm 3.0\%$ as the fractions of $\mathrm{B^0_{d,s}}$ produced in the fragmentation of b quarks at LEP, in

Decay mode	σ (MeV)	ε (%)
$B^0_d \to J\eta \to \mu^+\mu^-\gamma\gamma$	88 ± 5	$6.2 \pm 0.1 \pm 0.4$
$B^0_d \to J\eta \to e^+e^-\gamma\gamma$	41 ± 2	$6.9 \pm 0.1 \pm 0.3$
$B^0_s \to J\eta \to \mu^+\mu^-\gamma\gamma$	93 ± 5	$7.0 \pm 0.1 \pm 0.2$
$B^0_s \to J\eta \to e^+e^-\gamma\gamma$	41 ± 2	$7.2 \pm 0.1 \pm 0.2$
$B^0_d \to J\pi^0 \to \mu^+\mu^-$cluster	106 ± 5	$8.9 \pm 0.2 \pm 0.4$
$B^0_d \to J\pi^0 \to e^+e^-$cluster	61 ± 2	$10.3 \pm 0.2 \pm 0.3$
$B^0_s \to J\pi^0 \to \mu^+\mu^-$cluster	103 ± 7	$8.2 \pm 0.2 \pm 0.4$
$B^0_s \to J\pi^0 \to e^+e^-$cluster	59 ± 2	$10.3 \pm 0.2 \pm 0.3$

Table 2: Resolutions of a Gaussian fit to the signal Monte Carlo invariant mass spectra and efficiencies for the decay modes under investigation. The first error on the efficiencies is statistical, the second systematic.

agreement with the available measurements [22], $\mathrm{Br}(\eta \to \gamma\gamma) = 38.8\%$, $\mathrm{Br}(\pi^0 \to \gamma\gamma) = 98.8\%$, $\mathrm{Br}(J \to e^+e^-) = 5.99\%$ and $\mathrm{Br}(J \to \mu^+\mu^-) = 5.97\%$ [23].

The errors on all the quantities used in the calculation of the limits have been taken into account by folding their Gaussian distribution with the Poisson distribution describing the number of expected events, obtaining the 90% confidence level upper limits reported in Table 3.

Decay mode	Upper limit
$B^0_d \to J\eta$	1.2×10^{-3}
$B^0_s \to J\eta$	3.8×10^{-3}
$B^0_d \to J\pi^0$	3.2×10^{-4}
$B^0_s \to J\pi^0$	1.2×10^{-3}

Table 3: 90% confidence level upper limits on the branching ratio of the exclusive $B^0_{d,s}$ decays to J and η or π^0.

Conclusions

A search for exclusive decays of B^0_d and B^0_s mesons has been performed in the channels $B^0_d \to J\eta$, $B^0_d \to J\pi^0$, $B^0_s \to J\eta$ and $B^0_s \to J\pi^0$. The data sample consisted of more than three and half million hadronic Z decays collected by the L3 experiment at LEP from 1991 through 1995. No candidate event has been observed and upper limits at 90% confidence level on the branching ratios have been set in the order of $10^{-3} - 10^{-4}$ and are reported in Table 3. No large enhancement with respect to theoretical predictions has been observed.

These are the first experimental limits on the channels $B^0_d \to J\eta$, $B^0_s \to J\eta$ and $B^0_s \to J\pi^0$.

Acknowledgements

We wish to express our gratitude to the CERN accelerator divisions for the excellent performance of the LEP machine. We acknowledge the contributions of all the engineers and technicians who have participated in the construction and maintenance of this experiment. Those of us who are not from member states thank CERN for its hospitality and help.

The L3 Collaboration:

M.Acciarri,[28] O.Adriani,[17] M.Aguilar-Benitez,[27] S.Ahlen,[11] B.Alpat,[35] J.Alcaraz,[27] G.Alemanni,[23] J.Allaby,[18] A.Aloisio,[30] G.Alverson,[12] M.G.Alviggi,[30] G.Ambrosi,[20] H.Anderhub,[50] V.P.Andreev,[39] T.Angelescu,[13] F.Anselmo,[9] D.Antreasyan,[9] A.Arefiev,[29] T.Azemoon,[3] T.Aziz,[10] P.Bagnaia,[38] L.Baksay,[45] R.C.Ball,[3] S.Banerjee,[10] K.Banicz,[47] R.Barillère,[18] L.Barone,[38] P.Bartalini,[35] A.Baschirotto,[28] M.Basile,[9] R.Battiston,[35] A.Bay,[23] F.Becattini,[17] U.Becker,[16] F.Behner,[50] J.Berdugo,[27] P.Berges,[16] B.Bertucci,[18] B.L.Betev,[50] S.Bhattacharya,[10] M.Biasini,[18] A.Biland,[50] G.M.Bilei,[35] J.J.Blaising,[18] S.C.Blyth,[36] G.J.Bobbink,[2] R.Bock,[1] A.Böhm,[1] B.Borgia,[38] A.Boucham,[4] D.Bourilkov,[50] M.Bourquin,[20] D.Boutigny,[4] J.G.Branson,[41] V.Brigljevic,[50] I.C.Brock,[36] A.Buffini,[17] A.Buijs,[46] J.D.Burger,[16] W.J.Burger,[20] J.Busenitz,[45] A.Buytenhuijs,[32] X.D.Cai,[16] M.Campanelli,[50] M.Capell,[16] G.Cara Romeo,[9] M.Caria,[35] G.Carlino,[4] A.M.Cartacci,[17] J.Casaus,[27] G.Castellini,[17] F.Cavallari,[38] N.Cavallo,[30] C.Cecchi,[20] M.Cerrada,[27] F.Cesaroni,[24] M.Chamizo,[27] A.Chan,[52] Y.H.Chang,[52] U.K.Chaturvedi,[19] M.Chemarin,[26] A.Chen,[52] G.Chen,[7] G.M.Chen,[7] H.F.Chen,[21] H.S.Chen,[7] M.Chen,[16] G.Chiefari,[30] C.Y.Chien,[5] M.T.Choi,[44] L.Cifarelli,[40] F.Cindolo,[9] C.Civinini,[17] I.Clare,[16] R.Clare,[16] H.O.Cohn,[33] G.Coignet,[4] A.P.Colijn,[2] N.Colino,[27] V.Commichau,[1] S.Costantini,[38] F.Cotorobai,[13] B.de la Cruz,[27] A.Csilling,[14] T.S.Dai,[16] R.D'Alessandro,[17] R.de Asmundis,[30] H.De Boeck,[32] A.Degré,[4] K.Deiters,[48] P.Denes,[37] F.DeNotaristefani,[38] D.DiBitonto,[45] M.Diemoz,[38] D.van Dierendonck,[2] F.Di Lodovico,[50] C.Dionisi,[38] M.Dittmar,[50] A.Dominguez,[41] A.Doria,[30] I.Dorne,[4] M.T.Dova,[19,♮] E.Drago,[30] D.Duchesneau,[4] P.Duinker,[2] I.Duran,[42] S.Dutta,[10] S.Easo,[35] Yu.Efremenko,[33] H.El Mamouni,[26] A.Engler,[36] F.J.Eppling,[16] F.C.Erné,[2] J.P.Ernenwein,[26] P.Extermann,[20] M.Fabre,[48] R.Faccini,[38] S.Falciano,[38] A.Favara,[17] J.Fay,[26] O.Fedin,[39] M.Felcini,[50] B.Fenyi,[45] T.Ferguson,[36] D.Fernandez,[27] F.Ferroni,[38] H.Fesefeldt,[1] E.Fiandrini,[35] J.H.Field,[20] F.Filthaut,[36] P.H.Fisher,[16] G.Forconi,[16] L.Fredj,[20] K.Freudenreich,[50] C.Furetta,[28] Yu.Galaktionov,[29,16] S.N.Ganguli,[10] P.Garcia-Abia,[27] S.S.Gau,[12] S.Gentile,[38] J.Gerald,[5] N.Gheordanescu,[13] S.Giagu,[38] S.Goldfarb,[23] J.Goldstein,[11] Z.F.Gong,[21] A.Gougas,[5] G.Gratta,[34] M.W.Gruenewald,[8] V.K.Gupta,[37] A.Gurtu,[10] L.J.Gutay,[47] B.Hartmann,[1] A.Hasan,[31] D.Hatzifotiadou,[9] T.Hebbeker,[8] A.Hervé,[18] W.C.van Hoek,[32] H.Hofer,[50] H.Hoorani,[20] S.R.Hou,[52] G.Hu,[5] V.Innocente,[18] H.Janssen,[4] K.Jenkes,[1] B.N.Jin,[7] L.W.Jones,[3] P.de Jong,[18] I.Josa-Mutuberria,[27] A.Kasser,[23] R.A.Khan,[19] D.Kamrad,[49] Yu.Kamyshkov,[33] J.S.Kapustinsky,[25] Y.Karyotakis,[4] M.Kaur,[19,◇] M.N.Kienzle-Focacci,[20] D.Kim,[5] J.K.Kim,[44] S.C.Kim,[44] Y.G.Kim,[44] W.W.Kinnison,[25] A.Kirkby,[34] D.Kirkby,[34] J.Kirkby,[18] D.Kiss,[14] W.Kittel,[32] A.Klimentov,[16,29] A.C.König,[32] I.Korolko,[29] V.Koutsenko,[16,29] R.W.Kraemer,[36] W.Krenz,[1] H.Kuijten,[32] A.Kunin,[16,29] P.Ladron de Guevara,[27] G.Landi,[17] C.Lapoint,[16] K.Lassila-Perini,[50] P.Laurikainen,[22] M.Lebeau,[18] A.Lebedev,[16] P.Lebrun,[26] P.Lecomte,[50] P.Lecoq,[18] P.Le Coultre,[50] J.S.Lee,[44] K.Y.Lee,[44] C.Leggett,[3] J.M.Le Goff,[18] R.Leiste,[49] E.Leonardi,[38] P.Levtchenko,[39] C.Li,[21] E.Lieb,[49] W.T.Lin,[52] F.L.Linde,[2,18] L.Lista,[30] Z.A.Liu,[7] W.Lohmann,[49] E.Longo,[38] W.Lu,[34] Y.S.Lu,[7] K.Lübelsmeyer,[1] C.Luci,[38] D.Luckey,[16] L.Luminari,[38] W.Lustermann,[48] W.G.Ma,[21] M.Maity,[10] G.Majumder,[10] L.Malgeri,[38] A.Malinin,[29] C.Maña,[27] S.Mangla,[10] P.Marchesini,[50] A.Marin,[11] J.P.Martin,[26] F.Marzano,[38] G.G.G.Massaro,[2] D.McNally,[18] S.Mele,[30] L.Merola,[30] M.Meschini,[17] W.J.Metzger,[32] M.von der Mey,[1] Y.Mi,[23] A.Mihul,[13] A.J.W.van Mil,[32] G.Mirabelli,[38] J.Mnich,[18] P.Molnar,[8] B.Monteleoni,[17] R.Moore,[3] S.Morganti,[38] T.Moulik,[10] R.Mount,[34] S.Müller,[1] F.Muheim,[20] E.Nagy,[14] S.Nahn,[16] M.Napolitano,[30] F.Nessi-Tedaldi,[50] H.Newman,[34] T.Niessen,[1] A.Nippe,[1] A.Nisati,[38] H.Nowak,[49] H.Opitz,[1] G.Organtini,[38] R.Ostonen,[22] D.Pandoulas,[1] S.Paoletti,[38] P.Paolucci,[30] H.K.Park,[36] G.Pascale,[38] G.Passaleva,[17] S.Patricelli,[30] T.Paul,[12] M.Pauluzzi,[35] C.Paus,[1] F.Pauss,[50] D.Peach,[18] Y.J.Pei,[1] S.Pensotti,[28] D.Perret-Gallix,[4] S.Petrak,[8] A.Pevsner,[5] D.Piccolo,[30] M.Pieri,[17] J.C.Pinto,[36] P.A.Piroué,[37] E.Pistolesi,[28] V.Plyaskin,[29] M.Pohl,[50] V.Pojidaev,[29,17] H.Postema,[16] N.Produit,[20] D.Prokofiev,[39] G.Rahal-Callot,[50] P.G.Rancoita,[28] M.Rattaggi,[28] G.Raven,[41] P.Razis,[31] K.Read,[33] D.Ren,[50] M.Rescigno,[38] S.Reucroft,[12] T.van Rhee,[46] S.Riemann,[49] B.C.Riemers,[47] K.Riles,[3] O.Rind,[3] S.Ro,[44] A.Robohm,[50] J.Rodin,[16] F.J.Rodriguez,[27] B.P.Roe,[3] L.Romero,[27] S.Rosier-Lees,[4] Ph.Rosselet,[23] W.van Rossum,[46] S.Roth,[1] J.A.Rubio,[18] H.Rykaczewski,[50] J.Salicio,[18] E.Sanchez,[27] A.Santocchia,[35] M.E.Sarakinos,[22] S.Sarkar,[10] M.Sassowsky,[1] G.Sauvage,[4] C.Schäfer,[1] V.Schegelsky,[39] S.Schmidt-Kaerst,[1] D.Schmitz,[1] P.Schmitz,[1] M.Schneegans,[4] N.Scholz,[50] H.Schopper,[51] D.J.Schotanus,[32] J.Schwenke,[1] G.Schwering,[1] C.Sciacca,[30] D.Sciarrino,[20] J.C.Sens,[52] L.Servoli,[35] S.Shevchenko,[34] N.Shivarov,[43] V.Shoutko,[29] J.Shukla,[25] E.Shumilov,[29] A.Shvorob,[34] T.Siedenburg,[1] D.Son,[44] A.Sopczak,[49] V.Soulimov,[30] B.Smith,[16] P.Spillantini,[17] M.Steuer,[16] D.P.Stickland,[37] H.Stone,[37] B.Stoyanov,[43] A.Straessner,[1] K.Strauch,[15] K.Sudhakar,[10] G.Sultanov,[19] L.Z.Sun,[21] G.F.Susinno,[20] H.Suter,[50] J.D.Swain,[19] X.W.Tang,[7] L.Tauscher,[6] L.Taylor,[12] Samuel C.C.Ting,[16] S.M.Ting,[16] M.Tonutti,[1] S.C.Tonwar,[10] J.Tóth,[14] C.Tully,[37] H.Tuchscherer,[45] K.L.Tung,[7] Y.Uchida,[16] J.Ulbricht,[50] U.Uwer,[18] E.Valente,[38] R.T.Van de Walle,[32] G.Vesztergombi,[14] I.Vetlitsky,[29] G.Viertel,[50] M.Vivargent,[4] R.Völkert,[49] H.Vogel,[36] H.Vogt,[49] I.Vorobiev,[29] A.A.Vorobyov,[39] A.Vorvolakos,[31] M.Wadhwa,[6] W.Wallraff,[1] J.C.Wang,[16] X.L.Wang,[21] Z.M.Wang,[21] A.Weber,[1] F.Wittgenstein,[18] S.X.Wu,[19] S.Wynhoff,[1] J.Xu,[11] Z.Z.Xu,[21] B.Z.Yang,[21] C.G.Yang,[7] X.Y.Yao,[7] J.B.Ye,[21] S.C.Yeh,[52] J.M.You,[36] An.Zalite,[39] Yu.Zalite,[39] P.Zemp,[50] Y.Zeng,[1] Z.Zhang,[7] Z.P.Zhang,[21] B.Zhou,[11] Y.Zhou,[3] G.Y.Zhu,[7] R.Y.Zhu,[34] A.Zichichi,[9,18,19] F.Ziegler.[49]

1 I. Physikalisches Institut, RWTH, D-52056 Aachen, FRG[§]
III. Physikalisches Institut, RWTH, D-52056 Aachen, FRG[§]
2 National Institute for High Energy Physics, NIKHEF, and University of Amsterdam, NL-1009 DB Amsterdam, The Netherlands
3 University of Michigan, Ann Arbor, MI 48109, USA
4 Laboratoire d'Annecy-le-Vieux de Physique des Particules, LAPP,IN2P3-CNRS, BP 110, F-74941 Annecy-le-Vieux CEDEX, France
5 Johns Hopkins University, Baltimore, MD 21218, USA
6 Institute of Physics, University of Basel, CH-4056 Basel, Switzerland
7 Institute of High Energy Physics, IHEP, 100039 Beijing, China[△]
8 Humboldt University, D-10099 Berlin, FRG[§]
9 INFN-Sezione di Bologna, I-40126 Bologna, Italy
10 Tata Institute of Fundamental Research, Bombay 400 005, India
11 Boston University, Boston, MA 02215, USA
12 Northeastern University, Boston, MA 02115, USA
13 Institute of Atomic Physics and University of Bucharest, R-76900 Bucharest, Romania
14 Central Research Institute for Physics of the Hungarian Academy of Sciences, H-1525 Budapest 114, Hungary[‡]
15 Harvard University, Cambridge, MA 02139, USA
16 Massachusetts Institute of Technology, Cambridge, MA 02139, USA
17 INFN Sezione di Firenze and University of Florence, I-50125 Florence, Italy
18 European Laboratory for Particle Physics, CERN, CH-1211 Geneva 23, Switzerland
19 World Laboratory, FBLJA Project, CH-1211 Geneva 23, Switzerland
20 University of Geneva, CH-1211 Geneva 4, Switzerland
21 Chinese University of Science and Technology, USTC, Hefei, Anhui 230 029, China[△]
22 SEFT, Research Institute for High Energy Physics, P.O. Box 9, SF-00014 Helsinki, Finland
23 University of Lausanne, CH-1015 Lausanne, Switzerland
24 INFN-Sezione di Lecce and Universitá Degli Studi di Lecce, I-73100 Lecce, Italy
25 Los Alamos National Laboratory, Los Alamos, NM 87544, USA
26 Institut de Physique Nucléaire de Lyon, IN2P3-CNRS,Université Claude Bernard, F-69622 Villeurbanne, France
27 Centro de Investigaciones Energeticas, Medioambientales y Tecnologicas, CIEMAT, E-28040 Madrid, Spain♭
28 INFN-Sezione di Milano, I-20133 Milan, Italy
29 Institute of Theoretical and Experimental Physics, ITEP, Moscow, Russia
30 INFN-Sezione di Napoli and University of Naples, I-80125 Naples, Italy
31 Department of Natural Sciences, University of Cyprus, Nicosia, Cyprus
32 University of Nymegen and NIKHEF, NL-6525 ED Nymegen, The Netherlands
33 Oak Ridge National Laboratory, Oak Ridge, TN 37831, USA
34 California Institute of Technology, Pasadena, CA 91125, USA
35 INFN-Sezione di Perugia and Universitá Degli Studi di Perugia, I-06100 Perugia, Italy
36 Carnegie Mellon University, Pittsburgh, PA 15213, USA
37 Princeton University, Princeton, NJ 08544, USA
38 INFN-Sezione di Roma and University of Rome, "La Sapienza", I-00185 Rome, Italy
39 Nuclear Physics Institute, St. Petersburg, Russia
40 University and INFN, Salerno, I-84100 Salerno, Italy
41 University of California, San Diego, CA 92093, USA
42 Dept. de Fisica de Particulas Elementales, Univ. de Santiago, E-15706 Santiago de Compostela, Spain
43 Bulgarian Academy of Sciences, Central Laboratory of Mechatronics and Instrumentation, BU-1113 Sofia, Bulgaria
44 Center for High Energy Physics, Korea Advanced Inst. of Sciences and Technology, 305-701 Taejon, Republic of Korea
45 University of Alabama, Tuscaloosa, AL 35486, USA
46 Utrecht University and NIKHEF, NL-3584 CB Utrecht, The Netherlands
47 Purdue University, West Lafayette, IN 47907, USA
48 Paul Scherrer Institut, PSI, CH-5232 Villigen, Switzerland
49 DESY-Institut für Hochenergiephysik, D-15738 Zeuthen, FRG
50 Eidgenössische Technische Hochschule, ETH Zürich, CH-8093 Zürich, Switzerland
51 University of Hamburg, D-22761 Hamburg, FRG
52 High Energy Physics Group, Taiwan, China
§ Supported by the German Bundesministerium für Bildung, Wissenschaft, Forschung und Technologie
‡ Supported by the Hungarian OTKA fund under contract number T14459.
♭ Supported also by the Comisión Interministerial de Ciencia y Technologı́a
♯ Also supported by CONICET and Universidad Nacional de La Plata, CC 67, 1900 La Plata, Argentina
◇ Also supported by Panjab University, Chandigarh-160014, India
△ Supported by the National Natural Science Foundation of China.

References

[1] CLEO Collab., J. P. Alexander *et al.*, Phys. Lett. **B341** (1995) 435;
CLEO Collab., J. P. Alexander *et al.*, Phys. Lett. **B347** (1995) 469 (erratum).

[2] M. Gourdin *et al.*, Phys. Rev. Lett. **73** (1994) 3355.

[3] A. Deandrea *et al.*, Phys. Lett. **B318** (1993) 549;
M. Bauer *et al.*, Z. Phys. **C 34** (1987) 103.

[4] R. P. Feynman, in Proceedings of the 1964 International School of Subnuclear Physics "Ettore Majorana", ed. A. Zichichi, (Academic, New York, 1965).

[5] C. Reader and N. Isgur, Phys. Rev. **D47** (1993) 1007.

[6] R. Aleksan *et al.*, Phys. Rev. **D51** (1995) 6235.

[7] ARGUS Collab., H. Albrecht *et al.*, Phys. Lett. **B340** (1994) 217.

[8] CDF Collab., F. Abe *et al.*, Phys. Rev. Lett. **75** (1995) 3068.

[9] CLEO Collab., M. S. Alam *et al.*, Phys. Rev. **D50** (1994) 43.

[10] A. N. Kamal and A. B. Santra, Preprint Alberta Thy-31-94.

[11] A. N. Kamal and F. M. Al-Shamali, Preprint Alberta Thy-12-96.

[12] L3 Collab., B. Adeva *et al.*, Nucl. Inst. Meth. **A 289** (1990) 35;
L3 Collab., O. Adriani *et al.*, Physics Reports **236** (1993) 1;
M. Acciarri *et al.*, Nucl. Inst. Meth. **A 351** (1994) 300;
A. Adam, Preprint CERN-PPE/96-97.

[13] L3 Collab., M. Acciarri *et al.*, Phys. Lett. **B328** (1994) 223.

[14] L3 Collab.,"Dilepton Resonance Production in Hadronic Z Decays", Contributed paper to ICHEP96, Warsaw 1996, Abstract No. pa05-046.

[15] T. Sjöstrand, Computer Physics Commun. **82** (1994) 74;
T. Sjöstrand, Preprint CERN-TH.7112/93.

[16] R. Brun et al.,"GEANT 3", CERN DD/EE/84-1 (Revised), September 1987.

[17] H. Fesefeldt, Preprint RWTH Aachen PITHA 85/02 (1985).

[18] C. Peterson *et al.*, Phys. Rev. **D27** (1983) 105.

[19] L3 Collab., M. Acciarri *et al.*, Phys. Lett. **B363** (1995) 127.

[20] L3 Collab., B. Adeva *et al.*, Z. Phys. **C 51** (1991) 179.

[21] L3 Collab., O. Adriani *et al.*, Phys. Lett. **B307** (1993) 237.

[22] OPAL Collab., R. Akers *et al.*, Z. Phys. **C 66** (1995) 555;
OPAL Collab., R. Akers *et al.*, Z. Phys. **C 67** (1995) 57;
ALEPH Collab., D. Buskulic *et al.*, Z. Phys. **C 69** (1996) 585;
ALEPH Collab., D. Buskulic *et al.*, Phys. Lett. **B359** (1995) 236.

[23] Particle Data Group, Phys. Rev. **D54** (1996) 1.

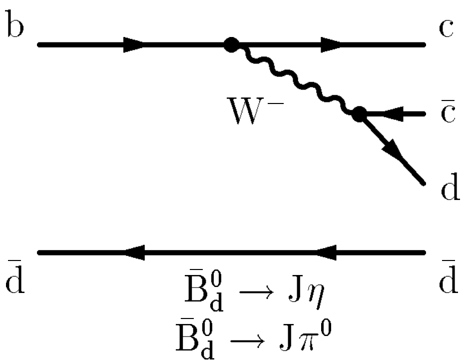

Figure 1: Feynman diagrams describing the processes $B^0_d \to J\eta$, $B^0_d \to J\pi^0$ and $B^0_s \to J\eta$.

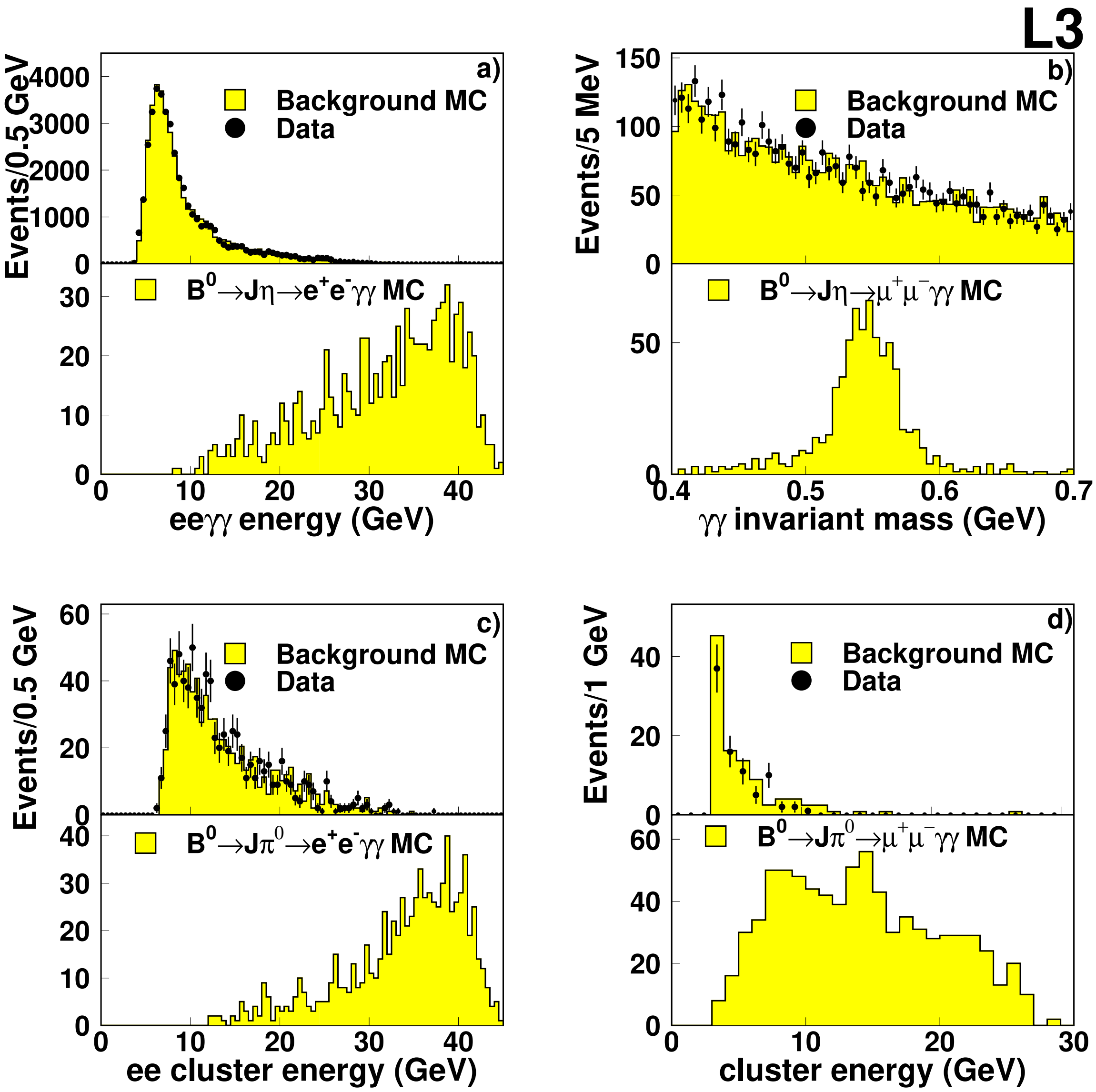

Figure 2: Some selection variables for exclusive B_d^0 decays for data and Monte Carlo simulations of the background (top part of any figure) and for the expected signal (bottom part of any figure). Preselection criteria are applied. a) Energy of the B candidate ($B_d^0 \to J\eta \to e^+e^-\gamma\gamma$). b) Invariant mass of η candidate ($B_d^0 \to J\eta \to \mu^+\mu^-\gamma\gamma$). c) Energy of the B candidate ($B_d^0 \to J\pi^0 \to e^+e^-$cluster). d) Energy of the π^0 candidate ($B_d^0 \to J\pi^0 \to \mu^+\mu^-$cluster). Variables shown in a) and c) are an example of the global kinematic selection, while the ones in b) and d) describe part of the light meson identification.

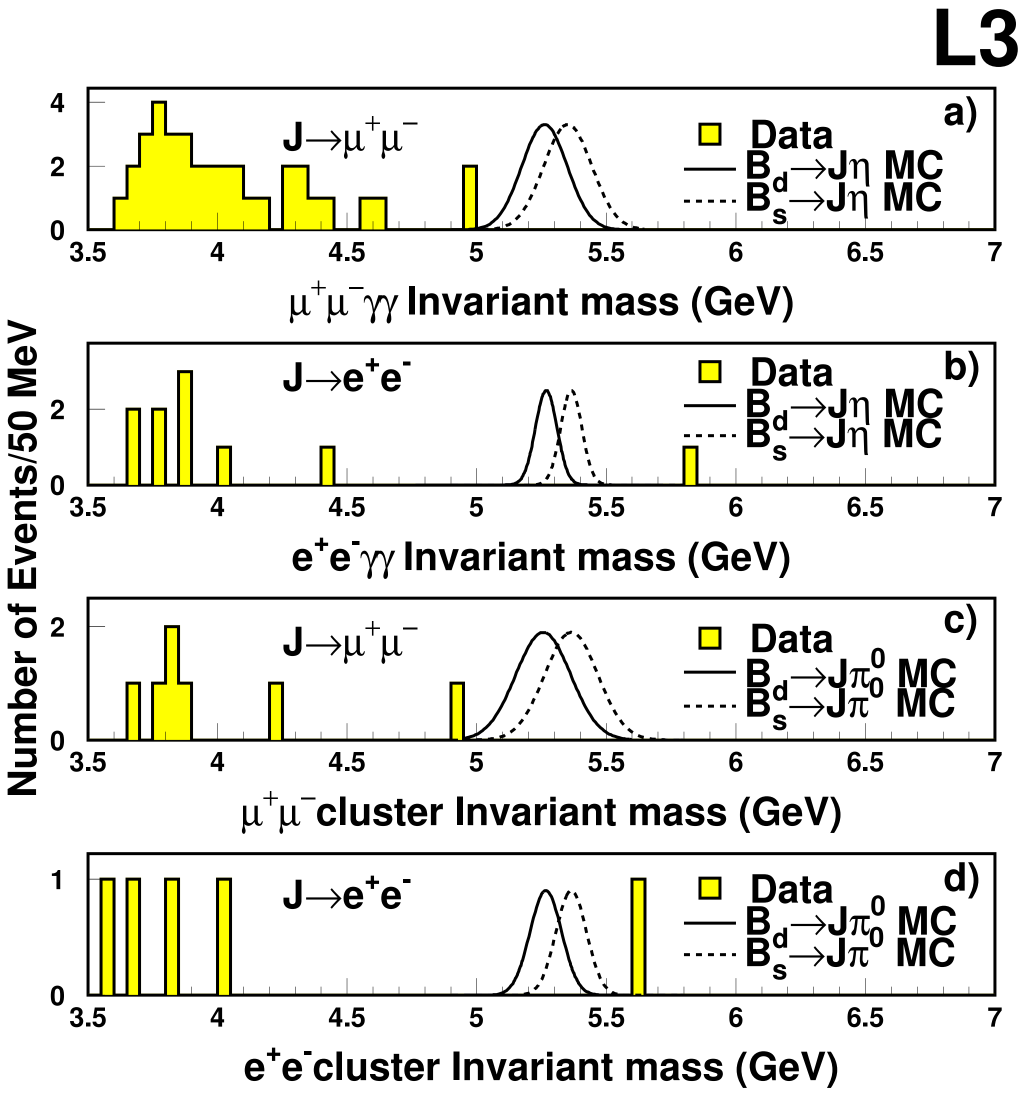

Figure 3: Invariant mass spectra for data (histogram) and the expected resolutions from the B^0_d (solid lines) and B^0_s (dashed lines) Monte Carlo (arbitrary units) after the application of the final cuts. a) $B^0_{d,s} \to J\eta \to \mu^+\mu^-\gamma\gamma$. b) $B^0_{d,s} \to J\eta \to e^+e^-\gamma\gamma$. c) $B^0_{d,s} \to J\pi^0 \to \mu^+\mu^-$cluster. d) $B^0_{d,s} \to J\pi^0 \to e^+e^-$cluster.